



ACADEMIC  
PRESS

BEST AVAILABLE COPY

Biochemical and Biophysical Research Communications 296 (2002) 313–318

BBRC

www.academicpress.com

## FAD-linked presenilin-1 mutants impede translation regulation under ER stress

Yuka Yasuda,<sup>a</sup> Takashi Kudo,<sup>a,\*</sup> Taiichi Katayama,<sup>b</sup> Kazunori Imaizumi,<sup>c</sup>  
Misako Yatera,<sup>a</sup> Masayasu Okochi,<sup>a</sup> Hidenaga Yamamori,<sup>a</sup> Naohiko Matsumoto,<sup>a</sup>  
Takayuki Kida,<sup>a</sup> Akio Fukumori,<sup>a</sup> Masayo Okumura,<sup>c</sup> Masaya Tohyama,<sup>b</sup>  
and Masatoshi Takeda<sup>a</sup>

<sup>a</sup> Division of Psychiatry and Behavioral Proteomics, Department of Post-Genomics and Diseases, Course of Advanced Medicine, Graduate School of Medicine, Osaka University, 2-2, Yamadaoka, Suita, Osaka 565-0871, Japan

<sup>b</sup> Department of Anatomy and Neuroscience, Graduate School of Medicine, Osaka University, 2-2, Yamadaoka, Suita, Osaka 565-0871, Japan

<sup>c</sup> Division of Structural Cell Biology, Nara Institute of Science and Technology (NAIST), 8916-5 Takayama, Ikoma, Nara 630-0101, Japan

Received 8 July 2002

### Abstract

FAD mutations in presenilin-1 (PS1) cause attenuation of the induction of the endoplasmic reticulum (ER)-resident chaperone GRP78/BiP under ER stress, due to disturbed function of IRE1, the sensor for accumulation of unfolded protein in the ER lumen. PERK, an ER-resident transmembrane protein kinase, is also a sensor for the unfolded protein response (UPR), causing phosphorylation of eukaryotic initiation factor 2 $\alpha$  (eIF2 $\alpha$ ) to inhibit translation initiation. Here, we report that the FAD mutant PS1 disturbs the UPR by attenuating both the activation of PERK and the phosphorylation of eIF2 $\alpha$ . Consistent with the results of a disturbed UPR, inhibition of protein synthesis under ER stress was impaired in cells expressing PS1 mutants. These results suggest that mutant PS1 impedes general translational attenuation regulated by PERK and eIF2 $\alpha$ , resulting in an increased load of newly synthesized proteins into the ER and subsequently increasing vulnerability to ER stress. © 2002 Elsevier Science (USA). All rights reserved.

**Keywords:** Familial Alzheimer's disease (FAD); Presenilin-1 (PS1); ER stress; Unfolded protein response (UPR); PERK; eIF2 $\alpha$

Alzheimer's disease (AD) is a progressive neurodegenerative disorder, characterized pathologically by extracellular amyloid plaques that are composed of the deposition of  $\beta$ -amyloid (A $\beta$ ) peptides of 40–42 residues and the formation of neurofibrillary tangles, major components of which are abnormally phosphorylated tau, in the brain. Some early-onset types of autosomal-dominant familial AD (FAD) are caused by mutations in the amyloid precursor protein (APP) [1,2], presenilin-1 (PS1) [3], or presenilin-2 (PS2) [4,5] genes. FAD-linked PS1 variants alter proteolytic processing and trafficking of APP [6,7]. Moreover, mutations in PS1 increase cellular susceptibility to apoptosis [8]. One interpretation, derived from cell culture studies, was that the PS1 mu-

tant perturbs subcellular calcium homeostasis in affected cells [9]. These statutes would impose a burden on the endoplasmic reticulum (ER). It has been reported that PS1 is localized in subcellular compartments and appears to be present in particularly high levels in the ER, the intermediate compartment, and the *cis*-Golgi region [8–10]. This has led us to study the relationship between ER function and PS1. Approximately one-third of all cellular proteins are translocated into the lumen of the ER, where post-translational modification, folding, and oligomerization occur. When cells are burdened with ER stress, malformed proteins accumulate in the ER, and specific pathways for cell survival are activated. These ER stress responses have been termed the unfolded protein response (UPR) [11–13]. Recently, several ER stress mediators for the UPR were identified in mammalian cells [11–13]. One of these mediators is an

\* Corresponding author. Fax: +81-6-6879-3059.

E-mail address: kudo@psy.med.osaka-u.ac.jp (T. Kudo).

ER-resident transmembrane kinase, IRE1. IRE1 senses the perturbed environment in the ER lumen and leads the signaling downstream to induce ER-resident chaperones such as GRP78/BiP, which facilitate protein folding [14]. This process was suggested to depend on oligomerization and autophosphorylation of IRE1 [14]. A second arm of the UPR consists of the suppression of protein translation. It has been suggested that reduced protein synthesis rates during ER stress serve to reduce the load of substrates presented to the folding machinery in the ER lumen. This correlates with enhanced phosphorylation of the  $\alpha$  subunit of eukaryotic translation initiation factor 2 (eIF2 $\alpha$ ) [15]. It was also reported that PERK-like ER kinase (PERK) participates in coupling ER stress to translation inhibition by phosphorylating eIF2 $\alpha$  [16,17]. The luminal domain of this kinase is related in sequence to that of IRE1 [17], suggesting that these kinases are simultaneously activated by the accumulation of misfolded proteins. We previously reported that the PS1 mutations found in patients with FAD led to attenuation of the induction of GRP78/BiP under ER stress conditions by inhibiting the phosphorylation of IRE1 [18]. In the present study, to analyze further the mechanism by which mutant PS1 downregulates the ER stress response, we examined whether PS1 mutants affect the signaling pathways mediated by another ER stress transducer, PERK.

## Materials and methods

**Expression plasmid and transfection.** Wild-type and  $\Delta$ E9 PS1 cDNAs were cloned into pcDNA3 (Invitrogen) as described previously [18]. Mouse Neuro2a (N2a) cells were transfected with each expression plasmid using lipofectamine 2000 (Gibco), and each stable transformant was established by G418 (Wako) selection.

**Culture of fibroblasts from PS1 mutant knock-in mice.** Primary fibroblasts were cultured from PS1 mutant (I213T) knock-in embryos on embryonic day 14.5, generated by mating heterozygous knock-in mice as described [19]. These cells were grown in DMEM supplemented with 10% fetal calf serum and were treated with 0.5 mM dithiothreitol (DTT) (Sigma) for specified times.

**Antibodies.** Rabbit antisera against a synthetic peptide corresponding to residues 1–14 of human PS1 have been previously described [18]. Anti-PERK antibody was raised against a synthetic peptide corresponding to residues of PERK (residues 1094–1114) and was affinity-purified using Prot On Kit1 (Multiple Peptide System, San Diego) [20]. Anti-KDEL monoclonal antibody, anti-PS1 monoclonal antibody, and anti-phosphorylated eIF2 $\alpha$  polyclonal antibodies were purchased from Stressgen, Chemicon, and Research Genetics Company, respectively.

**Fluorescent microscopy.** PS1-transfected N2a cells were fixed with 4% paraformaldehyde and permeabilized with 0.3% Triton X-100 for 10 min. The fixed cells were incubated with anti-PERK, anti-PS1, and/or anti-KDEL antibodies at dilutions of 1:500 for 5 h at 4°C and were stained with FITC-conjugated anti-rabbit IgG (Gibco) or Cy3-conjugated anti-rat IgG (Gibco) antibodies for 2 h. The stained cells were observed using a confocal microscope (Axioplan 2; Carl Zeiss).

**Induction of ER stress and Western blotting.** For Western blotting of PERK,  $3 \times 10^5$  N2a cells that were transfected with each PS1 construct were plated in 6-cm diameter dishes 2 days before the treatment with

the ER stress inducer, 1  $\mu$ M thapsigargin (Sigma). Sixty-percent confluent cultures were used to avoid various stresses induced by overgrowth and were placed in fresh media for more than 1 h before stress treatment with ER stressors. After being washed twice with ice-cold phosphate buffered saline (PBS), cells were lysed in 200  $\mu$ l of Triton buffer (20 mM HEPES, pH 7.5, 150 mM NaCl, 1% Triton X-100, 10% glycerol, 1 mM EDTA, 10 mM tetrasodium pyrophosphate, 100 mM NaF, 17.5 mM  $\beta$ -glycerophosphate, 1 mM phenylmethylsulfonyl fluoride (PMSF), 4 mg/ml aprotinin, and 2 mg/ml pepstatin A). All samples were centrifuged for 10 min at 4°C after being placed on ice for 1 h, and supernatants were collected. After the protein concentration of each sample was quantified using a bicinchoninic acid-based Protein Assay Kit (Pierce). Samples were loaded onto an SDS-polyacrylamide gel. Protein-equivalent samples were subjected to Western blotting. The ratio of phosphorylated PERK (P-PERK) signal to the total PERK signal and the intensity of the phosphorylated eIF2 $\alpha$  (P-eIF2 $\alpha$ ) in each lane were quantified densitometrically.

**Metabolic labeling.** To measure translational inhibition, sixty-percent confluent 6-cm diameter dishes of PS1-transfected N2a cells were washed twice with PBS and placed in 1.5 ml of serum-free ES media (Gibco BRL) containing 3 mg/L L-methionine and 4.8 mg/L L-cysteine. Cells were then pretreated for 20 min with or without 400 nM thapsigargin. The cells were pulse labeled for 10 min with 50  $\mu$ Ci of [ $^{35}$ S]methionine/cysteine express labeling mix (ICN Biochemicals) in methionine/cysteine-free DMEM containing 10% dialyzed fetal bovine serum, washed twice with ice-cold PBS containing unlabeled L-methionine (0.6 mg/ml) and L-cysteine (0.96 mg/ml), and lysed in 300  $\mu$ l of Triton buffer. The lysate was clarified by centrifugation, and 20  $\mu$ l was separated by SDS-PAGE. The gels were fixed, dried, and exposed for autoradiography. The levels of protein synthesis were quantified in four experiments by densitometry of autoradiogram films. The levels of [ $^{35}$ S] incorporation into proteins in the untreated cells were normalized to 100%.

## Results and discussion

Previously, we showed that FAD-linked PS1 mutants downregulate a signaling pathway of the UPR. This is caused by decreased levels of phosphorylated-IRE1, which activates transcription of molecular chaperones such as GRP78/BiP [18]. In the present study, we attempted to clarify whether the PS1 mutants influence the activation of PERK, another ER stress transducer, under ER stress conditions. The luminal domain of PERK is similar in sequence to that of IRE1 [18,21,22]. We established mouse N2a cells stably expressing wild-type PS1 or PS1 with an exon 9 deletion ( $\Delta$ E9) [23].

To investigate whether mutant PS1 ( $\Delta$ E9) influenced on the localization of PERK, we studied the subcellular localization of PS1 and PERK in N2a cells stably expressing wild-type PS1 and  $\Delta$ E9. Immunofluorescence microscopy showed that PS1 is preferentially distributed in the ER, Golgi, and cytoplasmic membrane, as described previously [24,25]. PERK was localized to the ER, as shown by the exclusive colocalization of PERK immunoreactivity with GRP78/BiP and GRP94, which are resident in the ER as detected by anti-KDEL antibody. Double labeling showed that in N2a cells overexpressing wild-type PS1, the immunoreactivity overlapped with that of PERK in the ER (data not

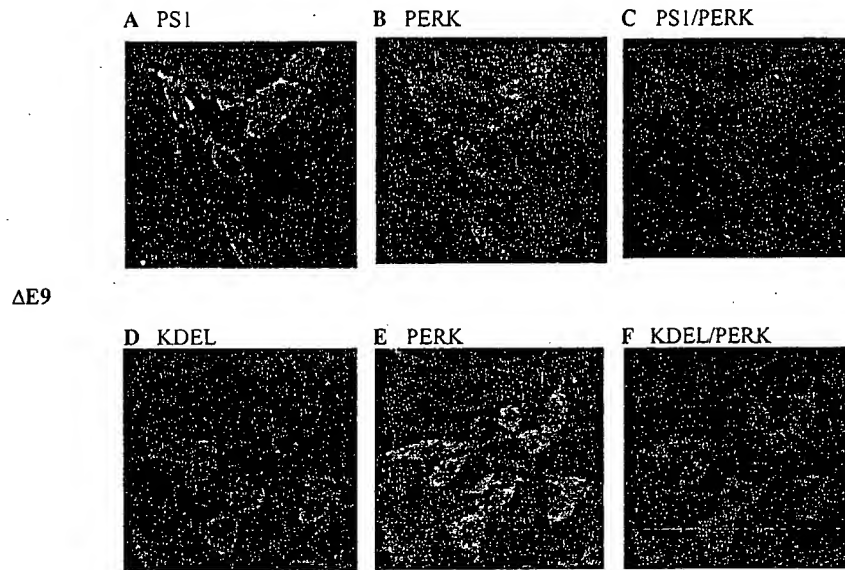


Fig. 1. Localization of PS1 in N2a cells with  $\Delta$  exon 9 mutant PS1 ( $\Delta$ E9) overlapped with that of the ER stress sensor PERK or GRP78/BiP, same as the cell with wild-type PS1. Immunostaining for PS1/PERK in the N2a cells. (A, PS1, red; B, PERK, green; C, overlapping, yellow.) D–F, Immunostaining for PS1/KDEL in the N2a cells. (D, PERK, green; E, KDEL, red; F, overlapping, yellow.) Anti-KDEL antibody detects both GRP78/BiP and GRP94 (as ER markers).

shown). A similar distribution was observed in the cells expressing the mutant PS1,  $\Delta$ E9 (Fig. 1), indicating that mutant PS1 does not alter the distribution of PERK in the ER.

We examined the response of PERK-eIF2 $\alpha$  signaling-pathway by ER stress in the N2a cells stably expressing mock, wild-type PS1, and  $\Delta$ E9. Before treatments with ER stressors, we pre-treated the cells with fresh medium

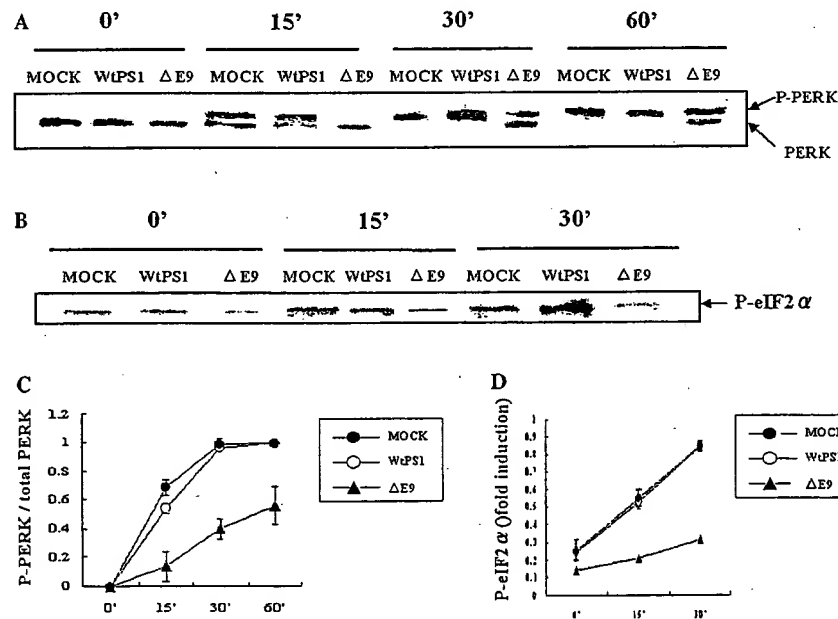


Fig. 2. PS1 mutant,  $\Delta$ E9, inhibits the activation of PERK and its downstream signal eIF2 $\alpha$  in N2a cells. Cells were stably transfected with each PS1 construct (MOCK, empty vector; wtPS1, wild-type PS1;  $\Delta$ E9,  $\Delta$  exon-9 mutant PS1). The cells were treated for the indicated periods of time with an agent that promotes ER stress, 1  $\mu$ M thapsigargin (Tg), after pretreatment. The cells were lysed in Triton buffer followed by Western blotting. (A) The blot was incubated with an antibody that detects both non-phosphorylated (inactive) PERK and the phosphorylated (activated) form of the protein (P-PERK). (B) The blot was incubated with an antibody specific to eIF2 $\alpha$  phosphorylated on serine 51 (P-eIF2 $\alpha$ ). (C) The ratio of phosphorylated PERK (P-PERK) to the total PERK signal of each lane in (A) was quantified densitometrically ( $n = 4$ ; means  $\pm$  SEM). (D) Fold inductions of phosphorylated eIF2 $\alpha$  (P-eIF2 $\alpha$ ) of each lane in (B) was quantified densitometrically ( $n = 4$ ; means  $\pm$  SEM).

for more than 1 h to obtain baseline data. After pre-incubation, the cells were exposed to 1  $\mu$ M thapsigargin, an inhibitor of the sarco-endoplasmic reticulum  $\text{Ca}^{2+}$ -ATPase (SERCA) pump (Fig. 2). Stress-induced activation of the protein kinase PERK stimulates phosphorylation PERK itself, which can be evaluated by a mobility shift of the PERK band upon SDS-PAGE [14], and the ratio of phosphorylated PERK (P-PERK) to the total PERK of each lane was analyzed densitometrically. Basal expression levels of PERK were not altered in N2a cell lines stably expressing each construct (Fig. 2A). In N2a cells transfected with empty vector (MOCK) or wild-type PS1, PERK completely underwent a shift in its mobility within 30 min after treatment with thapsigargin (Figs. 2A and C), suggesting that PERK was predominantly phosphorylated by the ER stressor in the cells with MOCK and wild-type PS1. In contrast, in cells expressing the PS1 mutant,  $\Delta$ E9, PERK was only partially phosphorylated, even 30 min after thapsigargin treatment (Figs. 2A and C). Furthermore, since PERK is an ER-resident transmembrane protein kinase that phosphorylates eIF2 $\alpha$  to downregulate protein synthesis under ER stress. Therefore, we examined the levels of phosphorylated-eIF2 $\alpha$  of the same lysates from N2a cells, quantifying these levels densitometrically. As was expected, in PS1 mutant-expressing cells, phosphorylation of eIF2 $\alpha$  was not complete within 15 min, whereas the phosphorylation occurred almost more immediately in cells with MOCK and wild-type PS1 than in mutant PS1 (Fig. 2B and D). We attempted the same experiments as described in Fig. 2 with another ER stress-inducing agent, DTT (1 mM), a reversible inhibitor of protein folding in the ER. The mutant PS1-expressing cells also retarded both the phosphorylation of PERK and the phosphorylation of eIF2 $\alpha$  by DTT (data not shown). These findings indicated that the PS1 mutation impairs the activation of PERK and subsequently inhibits the phosphorylation of eIF2 $\alpha$ .

To exclude the possibility that these phenomena were caused by overexpression of the PS1 mutation or that they were due to the unique mutation of PS1,  $\Delta$ E9, we studied primary cultured fibroblasts derived from embryos of PS1 mutant 'knock-in' mice that express mutant PS1 (I213T) [19]. Without ER stress, the total amount of PERK in fibroblasts from homozygous knock-in mice were similar in fibroblasts from the wild-type mice (Fig. 3). When we treated them with 0.5 mM DTT, the phosphorylation of PERK was disturbed in primary cultured fibroblasts from PS1 homozygous knock-in mice in comparison with that in fibroblasts from their wild-type littermates (Fig. 3). These results were completely consistent with those observed in the N2a cell lines. It is, therefore, clear that the mutations in PS1, not only  $\Delta$ E9, attenuate the activation of PERK under ER stress regardless of its expression level.

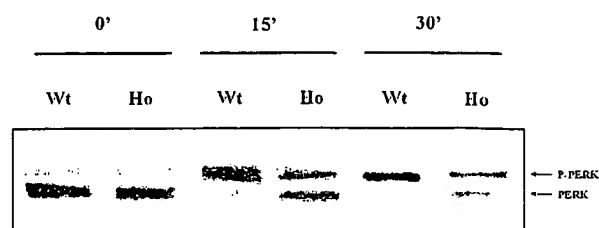


Fig. 3. Phosphorylation of PERK was impaired in primary cultured fibroblasts derived from PS1 mutant knock-in mice. Primary cultured fibroblasts from PS1 mutation (I213T) knock-in mice were treated with 0.5 mM dithiothreitol (DTT), which promotes ER stress, for the indicated periods after pretreatment. The cells were lysed in Triton buffer followed by Western blotting. The phosphorylation of PERK was disturbed in primary cultured fibroblasts from PS1 homozygous knock-in mice in comparison with that in fibroblasts from their wild-type littermates within 15 min of DTT treatment. (Wt, wild-type; Ho, homozygous mutant (I213T); P-PERK; phosphorylated PERK.)

The outcome of stimulation of the PERK-eIF2 $\alpha$  pathway is the attenuation of translation. We further confirmed whether the FAD-linked PS1 mutation actually influenced the regulation of translation when treated with agents that induce ER stress. N2a cells containing wild-type PS1 or mutant PS1 were cultured with or without 400 nM thapsigargin for 20 min and pulse-labeled for 10 min with [ $^{35}$ S]methionine/cysteine. N2a cells containing wild-type PS1 exhibited a profound attenuation in global translation rate. This is reflected in the reduced incorporation of [ $^{35}$ S]methionine/cysteine into cellular proteins following a short labeling pulse in the presence of ER stress-inducing agents. In contrast, the cells containing mutant PS1 did not reduce their translation rate when exposed to thapsigargin (Fig. 4). A recent study showed that *Perk* $^{-/-}$  cells have impaired attenuation of protein synthesis under ER stress and

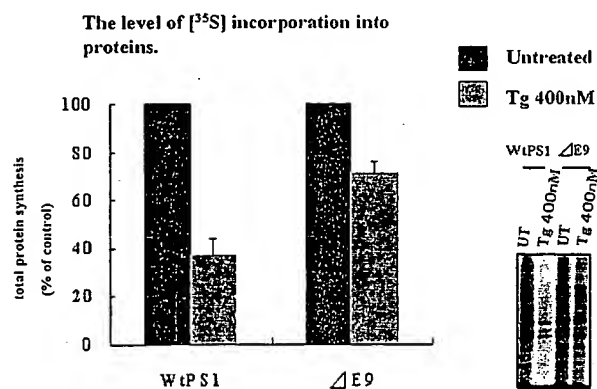


Fig. 4. Protein synthesis rates were studied by the incorporation of [ $^{35}$ S]methionine/cysteine into proteins during 10 min of pulse labeling that is followed by 20 min of exposure to thapsigargin (400 nM). Total protein synthesis level in 30 min was more suppressed in the cells with wild-type PS1 than  $\Delta$ E9. The levels of protein synthesis were quantified by densitometry of autoradiograms. The level of [ $^{35}$ S] incorporation into proteins in the untreated cells was normalized to 100% ( $n = 4$ ; means  $\pm$  SEM). The inset shows the representative autoradiograms.

that PERK is essential to translational regulation and cell survival during the UPR [22]. Our results showed that mutant PS1 disturbs the regulation of protein synthesis levels through the signaling pathway of PERK and eIF2 $\alpha$  and may result in impediment of cell survival.

However, it remains unclear how mutant PS1 inhibits the activation of ER stress transducers. Recently, it was proposed that activation of the ER stress transducers could be triggered by dissociation of GRP78/BiP from the stress transducers per se [14]. The dissociation leads to oligomerization of stress transducers inducing its autophosphorylation and then activation of downstream signaling. If PS1 mutants form misfolded structures, GRP78/BiP may inevitably bind to PS1 molecules to promote their folding. The formation of a complex of mutant PS1, PERK (or IRE1), and GRP78/BiP may inhibit the dissociation of GRP78/BiP from PERK or IRE1 under ER stress.

It is possible that PERK may associate with mutant PS1 as well as wild-type PS1 in the ER. However, it is unknown whether mutant PS1, which may be misfolded in the ER, associates with GRP78/BiP. Further study is needed to examine whether mutant PS1 inhibits the dissociation of GRP78/BiP from PERK during ER stress to clarify the mechanisms responsible for disturbed function of PERK by PS1 mutation.

In the brains of patients with Alzheimer's disease, A $\beta$  deposition is one of important pathologic features. FAD-linked PS1 mutants alter the processing of APP and increased the production of the more amyloidogenic A $\beta$  peptide, A $\beta$ 42 [6,7]. Therefore, whether the attenuation of the UPR causes the production of A $\beta$ 42 should be clarified. It has been reported that ER stress activates retrograde transport from the Golgi to the ER to prevent misfolded proteins from moving to targeted organelles [26]. Because the distribution of APP and its secretase affect the generation of A $\beta$ 42 [27], prolonged ER stress may shift their distribution to the ER and may change A $\beta$  production. Our current study showed that the PERK-eIF2 $\alpha$  pathway, as well as the IRE-GRP78/BiP pathway, is attenuated in cells with PS1 mutations. The disturbed UPR may prolong ER stress. These conditions may change A $\beta$  production and lead cells to apoptosis. It is uncertain whether disturbed UPR, which prolongs ER stress, accelerates A $\beta$  production. We are therefore currently analyzing A $\beta$  production in PERK knockout cells, whose UPR is attenuated under ER stress.

In conclusion, our findings suggest that the attenuation of the UPR by a PS1 mutations may be one of the pathologic processes in FAD.

#### Acknowledgment

This work was financially supported in part by the Gotoda foundation.

#### References

- [1] E.I. Rogaev, R. Sherrington, E.A. Rogaeva, G. Levesque, et al., Familial Alzheimer's disease in kinders with missense mutations in a gene on chromosome 1 related to the Alzheimer's disease type 3 gene, *Nature* 376 (1995) 775–778.
- [2] R. Sherrington, E.I. Rogaev, Y. Liang, E.A. Rogaeva, G. Levesque, et al., Cloning of a gene bearing missense mutations in early-onset familial Alzheimer's disease, *Nature* 375 (1995) 754–760.
- [3] P.H. St. George-Hyslop, J. Haines, E. Rogaev, M. Mortilla, G. Vaula, et al., Genetic evidence for a novel familial Alzheimer's disease locus on chromosome 14, *Nat. Genet.* 2 (1992) 330–334.
- [4] E. Levy-Lahad, E.M. Wijsman, E. Nemens, L. Anderson, et al., A familial Alzheimer's disease locus on chromosome 1, *Science* 269 (1995) 970–973.
- [5] E. Levy-Lahad, W. Wasco, P.D.M. Poorkaj, et al., Candidate gene for the chromosome 1 familial Alzheimer's disease locus, *Science* 269 (1995) 973–977.
- [6] D.R. Borchelt, G. Thinakaran, C.B. Eckman, et al., Familial Alzheimer's disease-linked presenilin 1 variants elevate A $\beta$ 1–42/1–40 ratio in vitro and in vivo, *Neuron* 17 (1996) 1005–1013.
- [7] C. Duff, K. Eckman, C. Zehr, et al., Increased amyloid- $\beta$ 42(43) in brains of mice expressing mutant presenilin 1, *Nature* 383 (1996) 710–713.
- [8] J. Walter, A. Capell, J. Grunberg, et al., The Alzheimer's disease-associated presenilins are differentially phosphorylated proteins located predominantly within the endoplasmic reticulum, *Mol. Med.* 2 (1996) 673–691.
- [9] J.G. Culvenor, F. Maher, G. Evin, et al., Alzheimer's disease-associated presenilin 1 in neuronal cells: evidence for localization to the endoplasmic reticulum-Golgi intermediate compartment, *J. Neurosci. Res.* 49 (1997) 719–731.
- [10] W.G. Annaert, L. Levesque, K. Craessaerts, et al., Presenilin 1 controls  $\gamma$ -secretase processing of amyloid precursor protein in pre-golgi compartments of hippocampal neurons, *J. Cell Biol.* 147 (1999) 277–294.
- [11] R.J. Kaufman, Stress signaling from the lumen of the endoplasmic reticulum: coordination of gene transcriptional and translational controls, *Genes Dev.* 13 (1999) 1211–1233.
- [12] K. Mori, Tripartite management of unfolded proteins in the endoplasmic reticulum, *Cell* 101 (2000) 451–454.
- [13] C.O. Brostrom, M.A. Brostrom, Regulation of translational initiation during cellular responses to stress, *Prog. Nucleic Acid Res. Mol. Biol.* 58 (1998) 79–125.
- [14] A. Bertolotti, Y. Zang, L.M. Hendershot, H.P. Harding, D. Ron, Dynamic interaction of BiP and ER stress transducers in the unfolded protein response, *Nat. Cell. Biol.* 2 (2000) 326–332.
- [15] Y. Shi et al., Identification and characterization of pancreatic eukaryotic initiation factor 2  $\alpha$ -subunit kinase, PEK, involved in translational control, *Mol. Cell Biol.* 18 (1998) 7499–7509.
- [16] C.R. Prostko, M.A. Brostrom, C.O. Brostrom, Reversible phosphorylation of eukaryotic initiation factor 2 $\alpha$  in response to endoplasmic reticular signaling, *Mol. Cell. Biochem.* 127–128 (1993) 255–256.
- [17] H.P. Harding, Y. Zhang, D. Ron, Protein translation and folding are coupled by an endoplasmic-reticulum-resident kinase, *Nature* 397 (1999) 21.
- [18] T. Katayama, K. Imaizumi, N. Sato, K. Miyoshi, T. Kudo, et al., Presenilin-1 mutations downregulate the signaling pathway of the unfolded protein response, *Nat. Cell. Biol.* 1 (1999) 479–485.
- [19] Y. Nakano, G. Kondoh, T. Kudo, K. Imaizumi, M. Kato, J.I. Miyazaki, M. Tohyama, J. Takeda, M. Takeda, Accumulation of murine amyloid  $\beta$ 42 with a gene-dosage dependent manner in PS1 'knock-in' mice, *Eur. J. Neurosci.* 11 (1999) 2577–2581.
- [20] T. Katayama, K. Imaizumi, A. Honda, T. Yoneda, T. Kudo, et al., Disturbed activation of endoplasmic reticulum stress transducers

- by familial Alzheimer's disease-linked presenilin-1 mutations, *J. Biol. Chem.* 16 (2001) 43446–43454.
- [21] H.P. Harding, I. Novoa, Y. Zhang, H. Zeng, M. Schapira, D. Ron, Regulated translation initiation controls stress-induced gene expression in mammalian cells, *Mol. Cell.* 6 (2000) 1099–1108.
- [22] H.P. Harding, Y. Zhang, A. Bertolotti, H. Zeng, D. Ron, PERK is essential for translational regulation and cell survival during the unfolded protein response, *Mol. Cell.* 5 (2000) 897–904.
- [23] J.P. Tur, S. Froelich, G. Prihar, R. Crook, M. Baker, et al., A mutation in Alzheimer's disease destroying a splice acceptor site in the presenilin-1 gene, *Neuroreport* 7 (1995) 297–301.
- [24] Q. Guo, B.L. Sopher, K. Furukawa, D.G. Pham, N. Robinson, et al., Alzheimer's Presenilin mutation sensitizes neural cells to apoptosis induced by trophic factor withdrawal and amyloid  $\beta$ -peptide: involvement of calcium and oxyradicals, *J. Neurosci.* 1 (1997) 4212–4222.
- [25] Nazneen, N. Dewji, S.J. Singer, The seven-transmembrane spanning topography of Alzheimer's disease-related presenilin proteins in the plasma membranes of cultured cells, *Proc. Natl. Acad. Sci. USA* 94 (1997) 14025–14030.
- [26] C. Hammond, A. Helenius, Quality control in the secretory pathway: retention of a misfolded viral membrane glycoprotein involves cycling between the ER, intermediate compartment, and Golgi apparatus, *J. Cell Biol.* 126 (1994) 41–52.
- [27] D.G. Cook, M.S. Forman, J.C. Sung, S. Leight, D.L. Kolson, T.I. Watsubo, V.M. Lee, R.W. Doms, Alzheimer's A $\beta$ (1–42) is generated in the endoplasmic reticulum/intermediate compartment of NT2N cells, *Nat. Med.* 3 (1997) 1021–1023.

## Disturbed Activation of Endoplasmic Reticulum Stress Transducers by Familial Alzheimer's Disease-linked Presenilin-1 Mutations\*

Received for publication, May 7, 2001, and in revised form, September 6, 2001  
Published, JBC Papers in Press, September 10, 2001, DOI 10.1074/jbc.M104096200

Taiichi Katayama†§¶, Kazunori Imaizumi¶\*\*‡, Akiko Honda†§¶, Takunari Yoneda†§, Takashi Kudo§§, Masatoshi Takeda§§, Kazutoshi Mori¶¶, Richard Rozmahel|||, Paul Fraser|||, Peter St. George-Hyslop|||, and Masaya Tohyama†§

From the †Department of Anatomy and Neuroscience, Graduate School of Medicine, Osaka University, 2-2 Yamadaoka, Suita, Osaka 565-0871, Japan, \*\*Division of Structural Cell Biology, Nara Institute of Science and Technology (NAIST), 8916-5 Takayama, Ikoma, Nara 630-0101, Japan, ‡Discovery Research Laboratory, Tanabe Seiyaku Co. Ltd., 3-16-89 Kashima, Yodogawaku, Osaka 532-0031, Japan, §§Department of Clinical Neuroscience, Psychiatry, Graduate School of Medicine, Osaka University, 2-2 Yamadaoka, Suita, Osaka 565-0871, Japan, ¶¶Graduate School of Biostudies, Kyoto University, 46-29 Yoshida-Shimoadachi, Sakyo-ku, Kyoto 606-8304, Japan, |||Center for Research into Neurodegenerative Diseases, Department of Medicine (Neurology), University of Toronto, Toronto, Ontario, M5S 1A8, Canada, and §CREST of Japan Science and Technology Corporation (JST), Kawaguchi, Saitama 332-0012, Japan

Recent studies have shown independently that presenilin-1 (PS1) null mutants and familial Alzheimer's disease (FAD)-linked mutants should both down-regulate signaling of the unfolded protein response (UPR). However, it is difficult to accept that both mutants possess the same effects on the UPR. Furthermore, contrary to these observations, neither loss of PS1 and PS2 function nor expression of FAD-linked PS1 mutants were reported to have a discernable impact on the UPR. Therefore, re-examination and detailed analyses are needed to clarify the relationship between PS1 function and UPR signaling. Here, we report that PS1/PS2 null and dominant negative PS1 mutants, which are mutated at aspartate residue 257 or 385, did not affect signaling of the UPR. In contrast, FAD-linked PS1 mutants were confirmed to disturb UPR signaling by inhibiting activation of both Ire1 $\alpha$  and ATF6, both of which are endoplasmic reticulum (ER) stress transducers in the UPR. Furthermore, PS1 mutants also disturbed activation of PERK (PKR-like ER kinase), which plays a crucial role in inhibiting translation during ER stress. Taken together, these observations suggested that PS1 mutations could affect signaling pathways controlled by each of the respective ER-stress transducers, possibly through a gain-of-function.

Alzheimer's disease is a progressive neurodegenerative disorder characterized pathologically by deposition of amyloid  $\beta$ -protein (A $\beta$ ),<sup>1</sup> formation of neurofibrillary tangles, and neuronal death in brain regions (1). Some cases show familial Alzheimer's disease (FAD), indicating that genetic factors are involved in the pathogenesis. A subset of early onset cases of FAD are caused by mutations in the amyloid precursor protein

(APP) gene located on chromosome 21 (2–4), presenilin-1 (PS1) found on chromosome 14 (5), and presenilin-2 (PS2) located on chromosome 1 (6–8). Mutations in the gene encoding PS1 are responsible for many cases of FAD. Although the mechanisms by which mutations in PS1 predispose individuals to FAD have not yet been determined, FAD-linked PS1 mutations have been shown to be associated with altered proteolytic processing of APP, such as increases in the production of the highly amyloidogenic A $\beta$  peptide, A $\beta$ 42 (9, 10). A $\beta$  production accompanied by the accumulation of carboxyl-terminal fragments of APP, which are generated by cleavage of  $\beta$ - and  $\gamma$ -secretases for APP, was inhibited in PS1-deficient cells (11). This finding indicated that PS1 is important in the  $\gamma$ -secretase-mediated cleavage process involved in generating A $\beta$ .

Mutations in PS1 increase cellular susceptibility to apoptosis induced by various insults, including the withdrawal of trophic factors and exposure to A $\beta$  (12, 13). Previously, we reported that the mechanism by which PS1 mutations promote cell death could contribute to increasing vulnerability to endoplasmic reticulum (ER) stress by altering the signaling pathway of the unfolded protein response (UPR) (14). The accumulation of misfolded polypeptides in the lumen of the ER results in activation of the UPR, inducing transcriptional up-regulation of genes encoding molecular chaperones and folding catalysts present in the ER (15). One of the mediators of the UPR is a transducer of ER stress, the ER-resident transmembrane kinase Ire1 (16, 17). Ire1 senses the perturbed environment in the ER and leads to downstream signaling by a process that is thought to depend on oligomerization and autophosphorylation of its kinase domain. The down-regulation of UPR signaling by PS1 mutations is caused by disruption of the function of Ire1, i.e. PS1 mutations decrease the levels of phosphorylated Ire1 (14). Recently, Niwa *et al.* (18) reported that PS1-deficient cells show a reduced ability to mount the UPR, with a reduction in nuclear accumulation of carboxyl-terminal fragments of Ire1. They speculated that impairment of the UPR is based on a defect in UPR-induced proteolytic processing of Ire1 at its intramembranous region by defects of  $\gamma$ -cleaving activities associated with PS1. Contrary to these observations, Sato *et al.* (19) have reported that neither PS1 null nor FAD-linked mutations affect the UPR signaling. Therefore, a re-examination and detailed analyses of relationships between PS1 functions and the UPR should be performed.

ATF6 is an ER transmembrane protein, recently isolated as

\* The costs of publication of this article were defrayed in part by the payment of page charges. This article must therefore be hereby marked "advertisement" in accordance with 18 U.S.C. Section 1734 solely to indicate this fact.

¶ These authors contributed equally to this work.

‡ To whom correspondence should be addressed. Tel.: 81-743-72-5411; Fax: 81-743-72-5419; E-mail: imaizumi@bs.aist-nara.ac.jp.

<sup>1</sup> The abbreviations used are: A $\beta$ , amyloid  $\beta$ -protein; APP, amyloid precursor protein; ER, endoplasmic reticulum; FAD, familial Alzheimer's disease; PS1 and -2, presenilin-1 and -2; UPR, unfolded protein response; eIF2 $\alpha$ , eukaryotic initiation factor-2 $\alpha$ ; Tm, tunicamycin; TG, thapsigargin; DTT, dithiothreitol; ATF6, activating transcription factor 6; PERK, PKR-like ER kinase; BiP, immunoglobulin-binding protein.



a possible mammalian UPR-specific transcription factor (20–22). ATF6 is cleaved at or close to the cytosolic face of the membrane in response to ER stress. The amino-terminal cytoplasmic domain, which contains the DNA-binding, dimerization, and transactivation domains, is translocated into the nucleus and activates transcription of ER molecular chaperone genes containing the ER stress response element (ERSE) (20, 23), which is thought to be a regulatory element of promoter regions conserved in ER molecular chaperone genes in mammalian cells. However, it has not been determined whether the luminal domain of ATF6 can itself sense the accumulation of unfolded proteins in the ER or whether cleavage of ATF6 requires ER stress-dependent activation of Ire1 proteins. If PS1 null or FAD-linked mutations affect the induction of ER molecular chaperones as described previously, these mutations could disturb the function of ATF6 as well as Ire1.

In the present study, to make it clear whether PS1 is associated with UPR signaling, we re-examined the effects of PS1 on induction of BiP/GRP78 mRNA and the ER stress response using PS1-deficient cells and cell lines expressing dominant negative PS1 mutants, with mutations of aspartate residues located in transmembrane domains 6 and 7 of PS1 (24), and expressing FAD-linked PS1 mutants. Furthermore, to clarify the mechanisms by which mutant PS1 down-regulates signaling of the UPR, we examined whether PS1 mutants affected the signaling pathways mediated by other ER stress transducers such as ATF6 or PKR-like ER kinase (PERK), which is an ER stress transducer and may play a role in inhibiting translation during ER stress (25, 26).

#### EXPERIMENTAL PROCEDURES

**Cell Culture and Induction of ER Stress**—Human neuroblastoma SK-N-SH cells and mouse embryonic fibroblasts were cultured in  $\alpha$ -minimal essential medium (Life Technologies, Inc.) supplemented with 10% fetal calf serum and Dulbecco's modified Eagle's medium (DMEM, Life Technologies, Inc.) supplemented with 20% fetal calf serum, respectively. Two days before the stimulation by various ER stressors,  $3 \times 10^5$  cells were plated in 10-cm-diameter dishes (for Western and Northern blotting analyses) or  $1 \times 10^5$  cells in 6-cm-diameter dishes (for cell death assay), with the media changed for fresh ones the next day. In all experiments of ER stress response, we used only culture dishes that were grown at 70–80% confluence to avoid various stresses induced by overgrowth. On the day of stimulation, cells were placed in fresh media for more than 1 h before treatment with ER stressors to create the same conditions in each dish. We used tunicamycin, thapsigargin, and DTT (all from Sigma) as ER stress inducers at indicated doses and times. The control dishes were treated by just changing the media.

Before collecting, cells were washed in ice-cold phosphate-buffered saline and then lysed in aliquots of 200  $\mu$ l of Triton buffer (20 mM HEPES, pH 7.5, 150 mM NaCl, 1% Triton X-100, 10% glycerol, 1 mM EDTA, 10 mM tetrasodium pyrophosphate, 100 mM NaF, 17.5 mM  $\beta$ -glycerophosphate, 1 mM phenylmethylsulfonyl fluoride, 4 mg/ml aprotinin, and 2 mg/ml pepstatin A) for detection of Ire1 $\alpha$  and PERK. For detection of ATF6, the cells were lysed in equal volumes of hot-SDS buffer (0.9% SDS, 15 mM EDTA, 8 mM methionine, and 1,000 units of Trasylol) were incubated in a boiling water bath for 10 min, cooled, diluted to 0.3% SDS, and adjusted to contain 33 mM Tris acetate, pH 8.5, and 1.7% Triton X-100. All samples were centrifuged at 4  $^{\circ}$ C for 10 min after standing on ice for 1 h, and then the supernatants were collected in 1.5-ml Eppendorf tubes.

**Antibodies**—Rabbit antisera against a synthetic peptide corresponding to residues 1–14 of human PS1 have been described previously (14). Anti-PERK antibody was raised against a synthetic peptide corresponding to residues of mouse PERK (residues 1094–1114) and was affinity-purified by ProtOn Kit1 (Multiple Peptide System, San Diego). Anti-ATF6 antibodies against recombinant ATF6 (amino acids 6–307) fused to *Escherichia coli* maltose-binding protein have also been described previously (21). Anti-Ire1 $\alpha$  antibodies were provided by Prof. D. Ron (New York University School of Medicine). Anti-phosphorylated eIF2 $\alpha$  polyclonal and anti- $\beta$ -actin monoclonal antibodies were purchased from Research Genetics Co. and Chemicon International Inc., respectively.

**Expression Plasmids and Gene Transfer into Cells**—Wild-type, A246E, and  $\Delta$ E9 PS1 cDNAs were cloned into pCDNA3 (Invitrogen) as

described previously (14). Human SK-N-SH neuroblastoma cells or mouse Neuro 2a cells were transfected with each expression plasmid using LipofectAMINE (Life Technologies, Inc.), and each stable transformant was established by selection with G418. Dominant negative PS1 mutants, which were mutated at aspartate residue 257 (D257A) or 385 (D385A), were cloned into pCDNA3.1/Zeo (Invitrogen) at *EcoRI* sites.

**Western Blotting**—For Western blotting of Ire1 $\alpha$  and PERK, cells were lysed in 1% Triton lysis buffer. Samples were loaded onto a 7% SDS-polyacrylamide gels. For Western blotting of ATF6, cells were lysed in Laemmli SDS sample buffer and then loaded onto 10% SDS-polyacrylamide gels. The protein concentration of each sample was quantified by Lowry assay (DC protein assay, Bio-Rad). Protein-equivalent samples were subjected to Western blotting. As an internal control, the levels of  $\beta$ -actin were examined on the same blot at the same time as the other proteins of interest.

**Northern Blotting**—Total RNA was extracted from cells treated with ER stress inducers. Aliquots of 10  $\mu$ g of each total RNA were fractionated by electrophoresis through 1.0% agarose-formaldehyde gels and transferred onto Immobilon-N membranes (Millipore, Bedford, MA). The membranes were hybridized with  $^{32}$ P-labeled human BiP cDNA probe. After washing in  $2\times$  SSC, 0.1% SDS and  $0.1\times$  SSC, 0.1% SDS, the membranes were dried and autoradiographed. The human BiP cDNA was a gift from Dr. S. Kaneda (Heat Shock Protein Research Institute).

**Fluorescence Microscopy**—Fibroblasts from PS1 mutant knock-in mice or SK-N-SH cells stably transfected with each PS1 construct were incubated with or without 3  $\mu$ g/ml Tm for the specified times. Cells were fixed in 4% paraformaldehyde and permeabilized in 0.3% Triton X-100. Anti-ATF6 antibody was used at a dilution of 1:1000. Stained cells were viewed with a confocal microscope (LSM 510, Carl Zeiss). To estimate the relative nuclear fluorescence intensity, cells were co-stained with 4,6-diamidino-2-phenylindole to demarcate the nuclear boundaries. Then, cytoplasmic (C), nuclear (N), or both (N/C) types of staining of ATF6 were measured independently in 10 fields. Each value was represented by the percentage of positive cells in each fraction, and the total of C, N, and N/C was 100%.

**Presenilin Null Mice**—Mice lacking functional expression of PS1 were generated using homologous recombination to introduce a neomycin cassette flanked by *loxP* sequences ~200 base pairs downstream of exon 5 of the murine PS1 gene. When the *loxP* flanked neomycin cassette is not removed by *cre* recombinase, the presence of cryptic splice sites within the neomycin cassette results in the generation of extremely low quantities of unstable transcripts lacking an open reading frame after exon 5.<sup>2</sup> These transcripts result in no detectable PS1 protein expression in embryonic stem cells or in the brains of animals homozygous for this construct. As expected, homozygous PS1-deficient mice (PS1<sup>-/-</sup>) displayed the previously reported skeletal abnormalities (27, 28). Embryonic fibroblasts from PS1/PS2 double homozygous-deficient mice (29) and the littermates were kindly provided by Dr. B. De Strooper.

**Culture of Fibroblasts from PS1-deficient and PS1 Mutant Knock-in Mice**—Primary fibroblasts were cultured from PS1<sup>+/-</sup> and PS1<sup>-/-</sup> embryos on embryonic day 14.5. Fibroblast cultures were also prepared from fetal mice at embryonic day 14.5, generated by mating heterozygous PS1 mutation (I213T) knock-in mice as described (30). These cells were grown in Dulbecco's modified Eagle's medium supplemented with 10% fetal calf serum and were treated with 2–3  $\mu$ g/ml Tm for the specified times. For evaluation of cell death, lactate dehydrogenase levels in culture medium were quantified as described previously (14).

#### RESULTS

**UPR Signaling in PS1 Mutant Cells**—PS1<sup>-/-</sup> cells have been reported to show impaired induction of BiP/GRP78, an ER molecular chaperone (18), suggesting that native PS1 is involved in UPR signaling. We re-examined the induction of BiP mRNA in PS1<sup>-/-</sup>, PS1/PS2<sup>-/-</sup> fibroblasts, and SK-N-SH cell lines expressing PS1 dominant negative mutants (D257A and D385A). The cells were stimulated with 3  $\mu$ g/ml tunicamycin (Tm), which induces ER stress by preventing protein glycosylation, for specified times. Northern blotting showed that there was no difference in the induction of BiP mRNA between

<sup>2</sup> R. Rozmahel, P. Fraser, and P. St. George-Hyslop, manuscript in preparation.



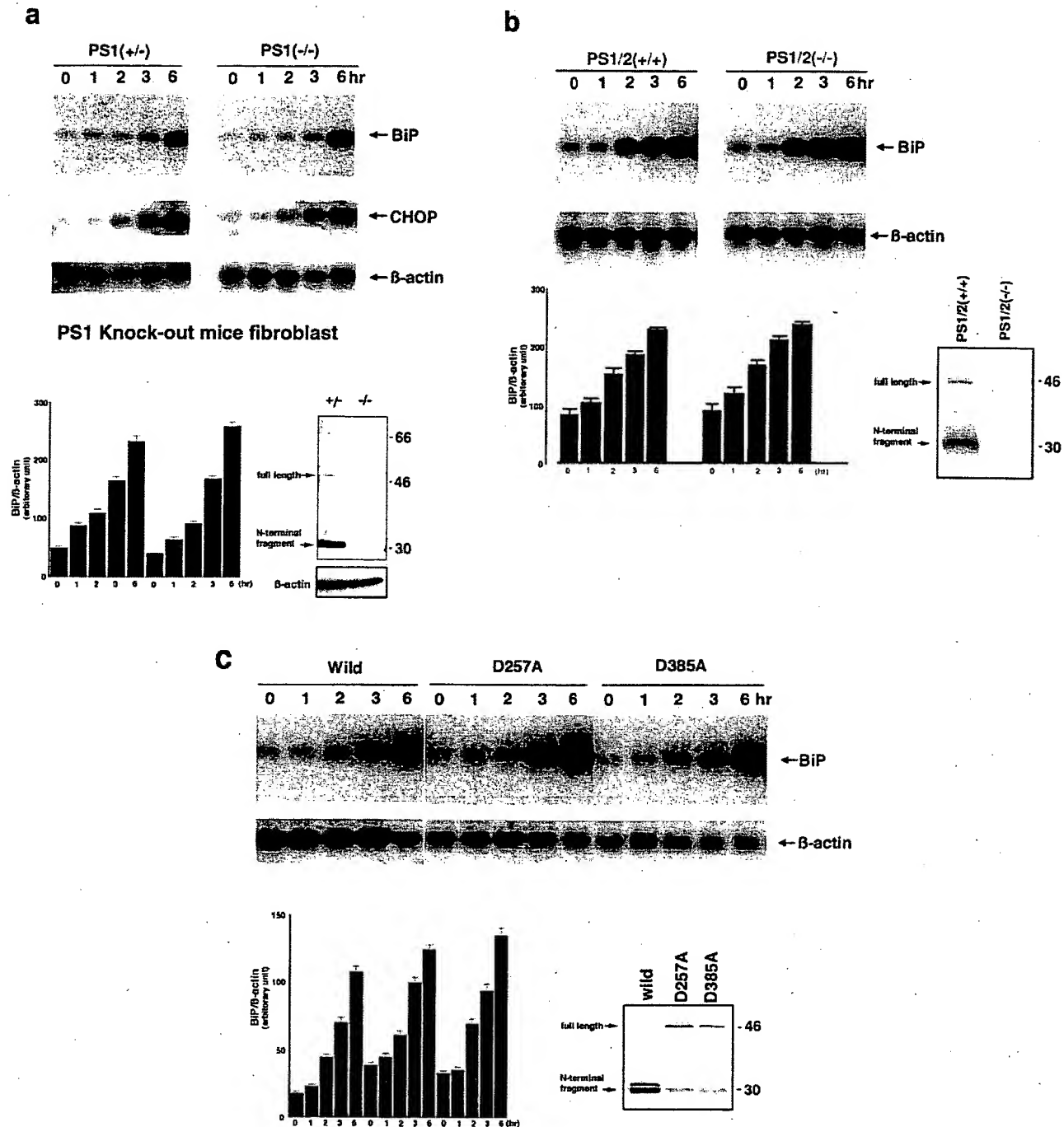


**FIG. 1. Induction of BiP mRNA in PS1<sup>-/-</sup> or PS1 dominant negative cells.** Northern blotting of BiP/GRP78 and CHOP mRNAs. Primary cultured fibroblasts from PS1<sup>+/-</sup> and <sup>-/-</sup> (a) and PS1/2<sup>+/+</sup> and <sup>-/-</sup> (b) mice were exposed to Tm at a concentration of 3  $\mu$ g/ml for the indicated times. Total RNA was isolated from each culture and subjected to Northern blotting with probes for BiP, CHOP, or  $\beta$ -actin mRNA. Lower panel, left, the amounts of BiP mRNA in each cell are shown. Quantitative analyses of BiP mRNA levels as shown in autoradiographs were performed as described previously (14). Values are arbitrary intensities and represent the mean  $\pm$  S.D. of data from four independent experiments. Right, the expression of PS1 in fibroblasts from PS1-deficient mice. Full-length and amino-terminal fragments of PS1 were absent in PS1-deficient cells. c, SK-N-SH cells were stably transfected with dominant negative PS1 mutants mutated at aspartate residues 257 or 385. Wild, cells stably transfected with wild-type PS1. The lower panel shows quantitative analyses of BiP mRNA levels as shown in autoradiographs and Western blotting of PS1 in these cells. Note that mutant cells showed accumulation of full-length PS1 (arrow).

PS1<sup>-/-</sup> and PS1<sup>+/-</sup> fibroblasts, PS1/PS2<sup>-/-</sup> and PS1/PS2<sup>+/+</sup> fibroblasts, or SK-N-SH cells expressing wild-type PS1 and dominant negative mutants (Fig. 1). No effects of these mutations on the induction of BiP mRNA were confirmed at concentrations from 0.5 to 10  $\mu$ g/ml of Tm. In contrast, fibroblasts from FAD-linked PS1 mutant knock-in mice, which express the PS1 mutant (I213T) at normal physiological levels (30), and

SK-N-SH cells expressing PS1 mutant (delta exon 9, PS1 $\Delta$ 9) revealed that the induction of BiP mRNA was delayed and attenuated compared with wild-type cells at each dose from 0.5 to 3  $\mu$ g/ml Tm (Fig. 2). Furthermore, we examined the changes in induction of CHOP, which is also induced during ER stress (31, 32). We detected no differences in the induction of CHOP mRNA in PS1<sup>-/-</sup> fibroblasts (Fig. 1) or aspartate mutant-

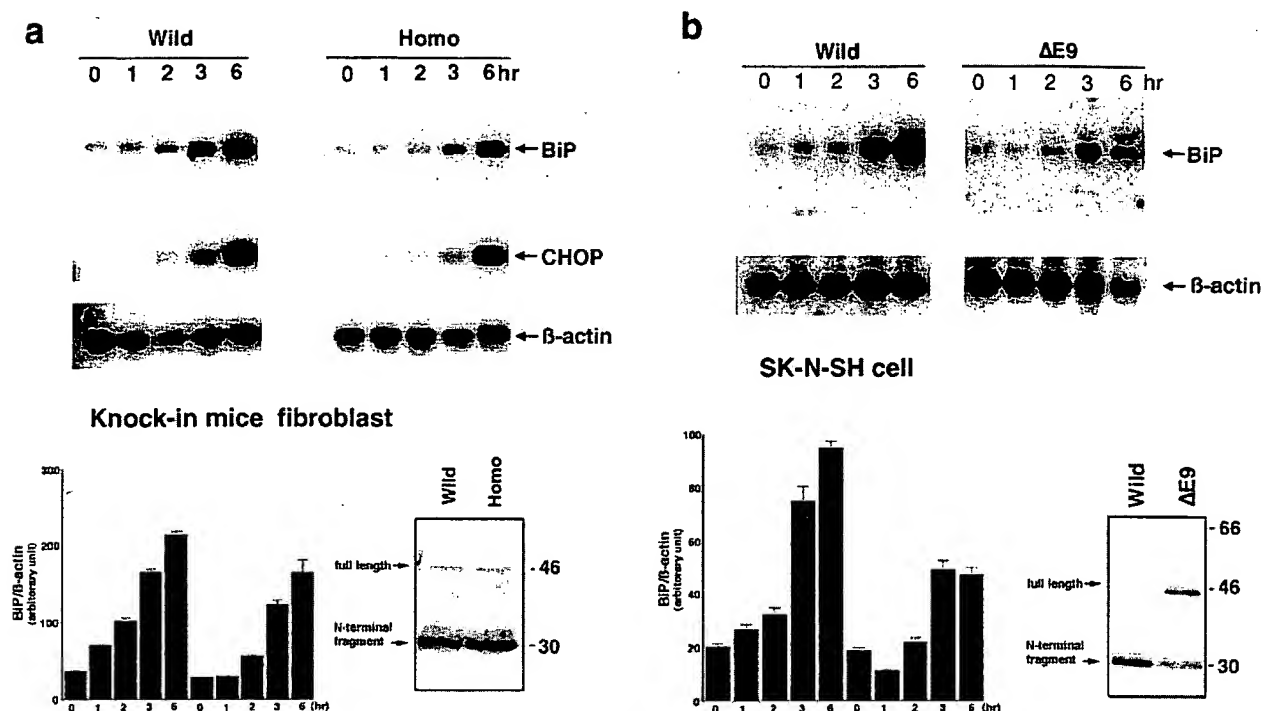


FIG. 2. BiP mRNA in PS1 mutation knock-in or transfected cells. *a*, primary cultured fibroblasts from PS1 mutation (*I213T*) knock-in mice (wild and homozygous (*Homo*)). Time courses of the levels of BiP, CHOP, and  $\beta$ -actin mRNA after treatment with Tm are shown. *b*, SK-N-SH cells were stably transfected with each PS1 construct (*Wild*, wild-type;  $\Delta E9$ , mutant deleted exon 9). Induction of BiP and/or CHOP mRNA was attenuated in homozygous fibroblasts and  $\Delta E9$ -expressing SK-N-SH cells when cells were treated with 3  $\mu$ g/ml Tm. These results were obtained for doses from 0.5 to 3  $\mu$ g/ml Tm.

expressing neuroblastomas (data not shown). Cells expressing FAD-linked PS1 mutants exhibited a delay in CHOP mRNA induction similar to that in BiP mRNA induction (Fig. 2). The effects of FAD-linked PS1 mutations on the induction of BiP and CHOP mRNA were observed at each dose of Tm from 0.5 to 5  $\mu$ g/ml, but they could not be detected at 10  $\mu$ g/ml because of the toxic effects of Tm, suggesting that higher doses of ER stress inducers could mask the down-regulation of UPR induced by PS1 mutation. Down-regulation of BiP mRNA induction by FAD-linked PS1 mutation was also observed in treatments with thapsigargin (TG) and dithiothreitol (DTT) (data not shown). These results indicated that although native PS1 is not involved in UPR signaling, FAD-linked PS1 mutants do have an effect that may be attributable to a gain of aberrant functions.

**Vulnerability to ER Stress in Cells Expressing PS1 Mutants**—We previously demonstrated that cells expressing PS1 mutants exhibited increased vulnerability to various ER stresses, the mechanism of which was the down-regulation of UPR signaling (14). If native PS1 is not relevant to UPR signaling, sensitivity to ER stress in PS1-deficient cells should be equivalent to that in wild-type cells. Therefore, we carried out cell death assays using various mutant cells treated with Tm. Cell death induced by Tm was significantly promoted in PS1 mutation knock-in fibroblasts and SK-N-SH cells expressing PS1 $\Delta 9$  (Fig. 3c), findings consistent with those observed previously. In contrast, PS1<sup>-/-</sup> fibroblasts and SK-N-SH cells expressing PS1 dominant negative mutants showed no differences in cell death induced by ER stress as compared with the respective controls (Fig. 3, *a* and *b*). Thus, we confirmed that a deficiency of PS1 does not affect susceptibility to ER stress and that native PS1 is not associated with UPR signaling.

**Mutant PS1 Alters Proteolytic Cleavage and Translocation of ATF6**—ATF6 is cleaved at or close to the cytosolic face of the membrane, and its amino-terminal portion is translocated into

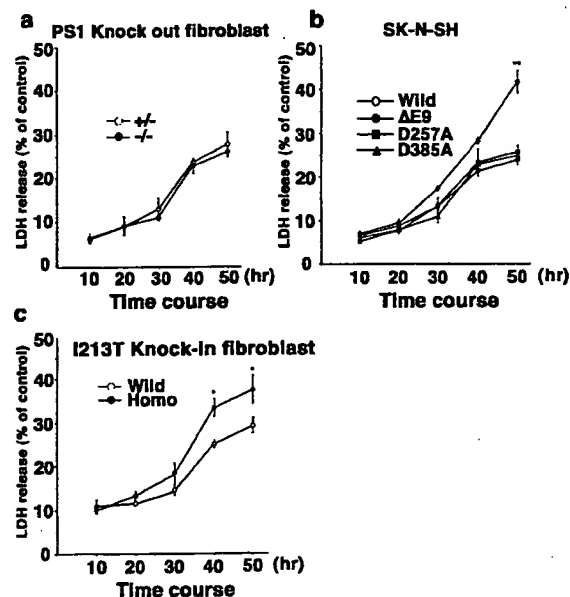
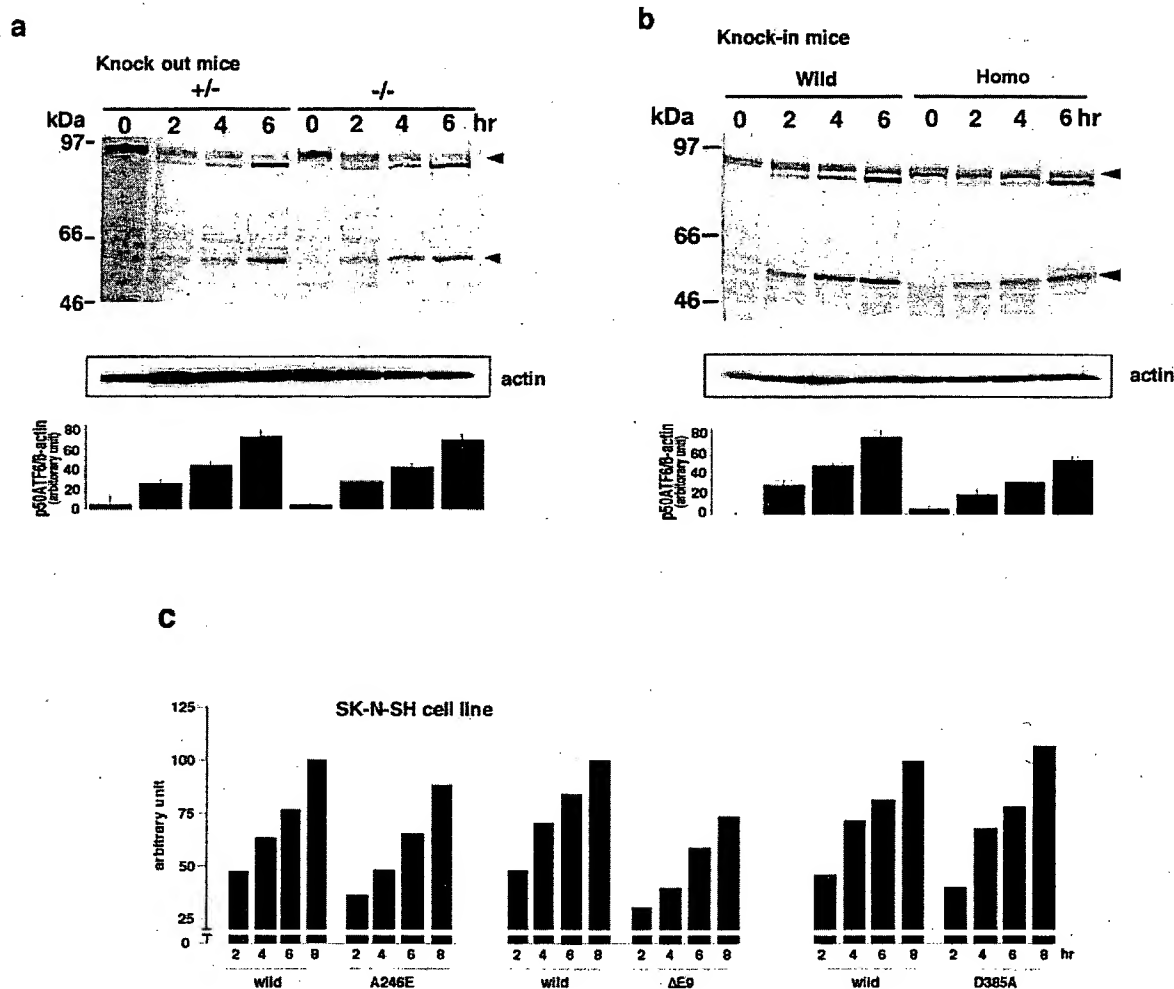


FIG. 3. Vulnerability to ER stress in each PS1 mutant-expressing cell. PS1-deficient fibroblasts (*a*), SK-N-SH cells stably transfected with each PS1 construct (*b*), and PS1 mutation (*I213T*) knock-in fibroblasts (*c*) were treated with Tm (fibroblasts, 3  $\mu$ g/ml; SK-N-SH cells, 0.5  $\mu$ g/ml) for the indicated times. Supernatants of each culture were collected, and the activities of released lactate dehydrogenase (LDH) were determined. The data are means  $\pm$  S.D. of four independent experiments. Only cells expressing FAD-linked PS1 mutations exhibited increased vulnerability to ER stress. \*,  $p < 0.05$ ; \*\*,  $p < 0.01$  relative to the controls (wild-type cells); significance was calculated by Student's *t* test.

the nucleus during ER stress. The amino-terminal domain activates transcription of ER molecular chaperones such as BiP and GRP94 (20, 21, 22). We examined whether FAD-linked PS1



**FIG. 4. Conversion of ATF6 to p50ATF6 after ER stress.** Primary cultured fibroblasts from PS1 knock-out (*a*) and PS1 mutation knock-in (*b*) mice were treated with 2  $\mu$ g/ml Tm for the indicated times, and cells were lysed as described under "Experimental Procedures." Then, aliquots of lysates were subjected to Western blotting of ATF6. Wild-type cells showed accumulation of p50ATF6 band (arrowhead) after treatment with Tm. *a*, the amounts of p50ATF6 in PS1<sup>-/-</sup> cells were almost equivalent to those in PS1<sup>+/-</sup> cells. *Middle panel*, Western blotting of  $\beta$ -actin. *Lower panel*, the amounts of accumulated p50ATF6 fragments were analyzed quantitatively and normalized to expression levels of  $\beta$ -actin protein. Values are arbitrary intensities and represent the mean  $\pm$  S.D. of data from four independent experiments. *b*, homozygous PS1 mutation knock-in cells (*Homo*) showed lower levels of p50ATF6 than those in wild-type cells at each time point. *c*, quantitative analysis of accumulated p50ATF6 fragments in each stable transfectant of SK-N-SH cells after treatment with Tm. FAD-linked PS1 mutation (A246E,  $\Delta$ E9)-expressing cells showed that the amounts of accumulated p50ATF6 fragments were decreased at each time point compared with wild type-expressing cells. Values are arbitrary intensities and represent the means  $\pm$  S.D. of data from four independent experiments.

mutants also impaired activation of the other UPR transducer protein, ATF6, similarly to Ire1 as has been reported previously (14). Fibroblasts from PS1 mutant knock-in mice were stimulated by the addition of 2  $\mu$ g/ml Tm. Cells were lysed, and Western blotting was performed using anti-ATF6 antibodies raised against the amino-terminal region of ATF6 (amino acids 6–307). ATF6 was constitutively expressed in wild-type fibroblasts as a 90-kDa protein (p90ATF6) (Fig. 4*b*). The p90ATF6 levels decreased, and instead a new band of 50-kDa (p50ATF6) appeared 2 h after treatment with Tm, with p50ATF6 gradually accumulating after this time. The homozygous fibroblasts from the PS1 mutant knock-in mice showed that the production of p50ATF6 was delayed and that the levels of the fragments were decreased by ~50% compared with those from wild-type mice from 2 to 6 h after treatment with Tm (Fig. 4*b*). We also confirmed that the conversion of p90ATF6 to p50ATF6 was inhibited in SK-N-SH neuroblastoma cells stably transfected with FAD-linked PS1 mutants, such as PS1 $\Delta$ 9 or PS1 with an alanine-to-glutamate mutation (A246E) (Fig. 4*c*). These findings indicated that PS1 mutations disturb the conversion of

ATF6 under conditions of ER stress. In contrast, these effects on ATF6 were not observed in either PS1-deficient cells (Fig. 4*a*) or in PS1 dominant negative-expressing cells (Fig. 4*c*). Thus, native PS1 is not considered to play a role in the processing of ATF6 at or close to the cytosolic face of the ER membrane, findings that are likely to be different in the case of processing at the  $\gamma$ -site of APP.

ATF6 has been reported to be constitutively expressed at the perinuclear region under non-ER stress conditions. ER stress causes the conversion of p90ATF6 to p50ATF6, which is translocated into the nucleus. We performed an immunocytochemical analysis of the subcellular localization of ATF6 in PS1 mutant cells under normal or ER stress conditions. For evaluation of ATF6 translocation, the fluorescence signals of cells stained with anti-ATF6 antibodies were divided into cytoplasmic (C), nuclear (N), or both regions (N/C). N/C shows that ATF6 was shifting from the ER to the nucleus (Fig. 5*a*). Under non-inducing conditions, the distribution of ATF6 (p90ATF6) in PS1 mutant knock-in cells resembled that seen in fibroblasts expressing wild-type PS1 (Fig. 5*b*). p90ATF6 was localized

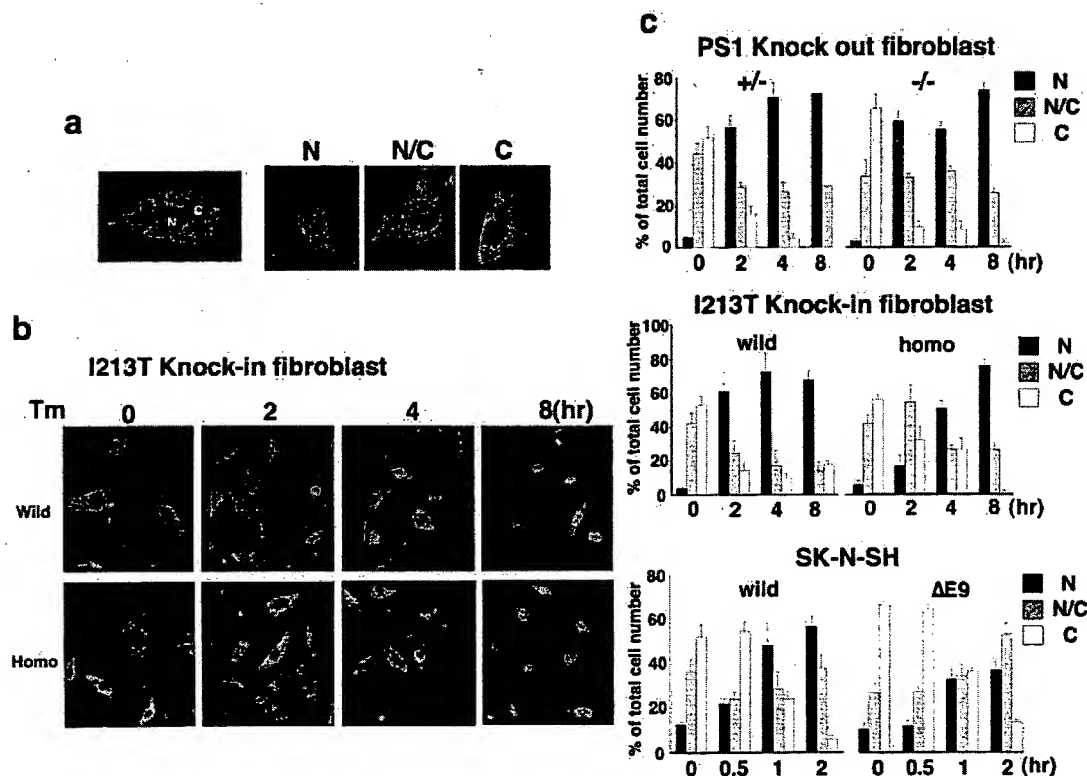


FIG. 5. Translocation of ATF6 into nuclei from the ER. *a*, left, immunoreactivity of ATF6 under non-ER stress conditions. *N*, nuclear; *C*, cytosolic. Right, immunoreactivity of ATF6 during ER stress. The fluorescence signals of cells stained with anti-ATF6 antibodies were divided into cytosolic (*C*), nuclear (*N*), or both regions (*N/C*) as described under "Experimental Procedures." *b*, PS1 mutation knock-in cells were exposed to Tm for the indicated times. Nuclear translocation of ATF6 fragments was delayed in homozygous cells (*Homo*) compared with that in wild-type cells (*Wild*). *c*, quantification of immunofluorescence of ATF6. Upper panel, PS1 knock-out fibroblast. Middle panel, PS1 mutation knock-in fibroblast. Lower panel, SK-N-SH cell lines. Values show the frequency of cells that were localized in each region. Values represent the means  $\pm$  S.D. as described under "Experimental Procedures."

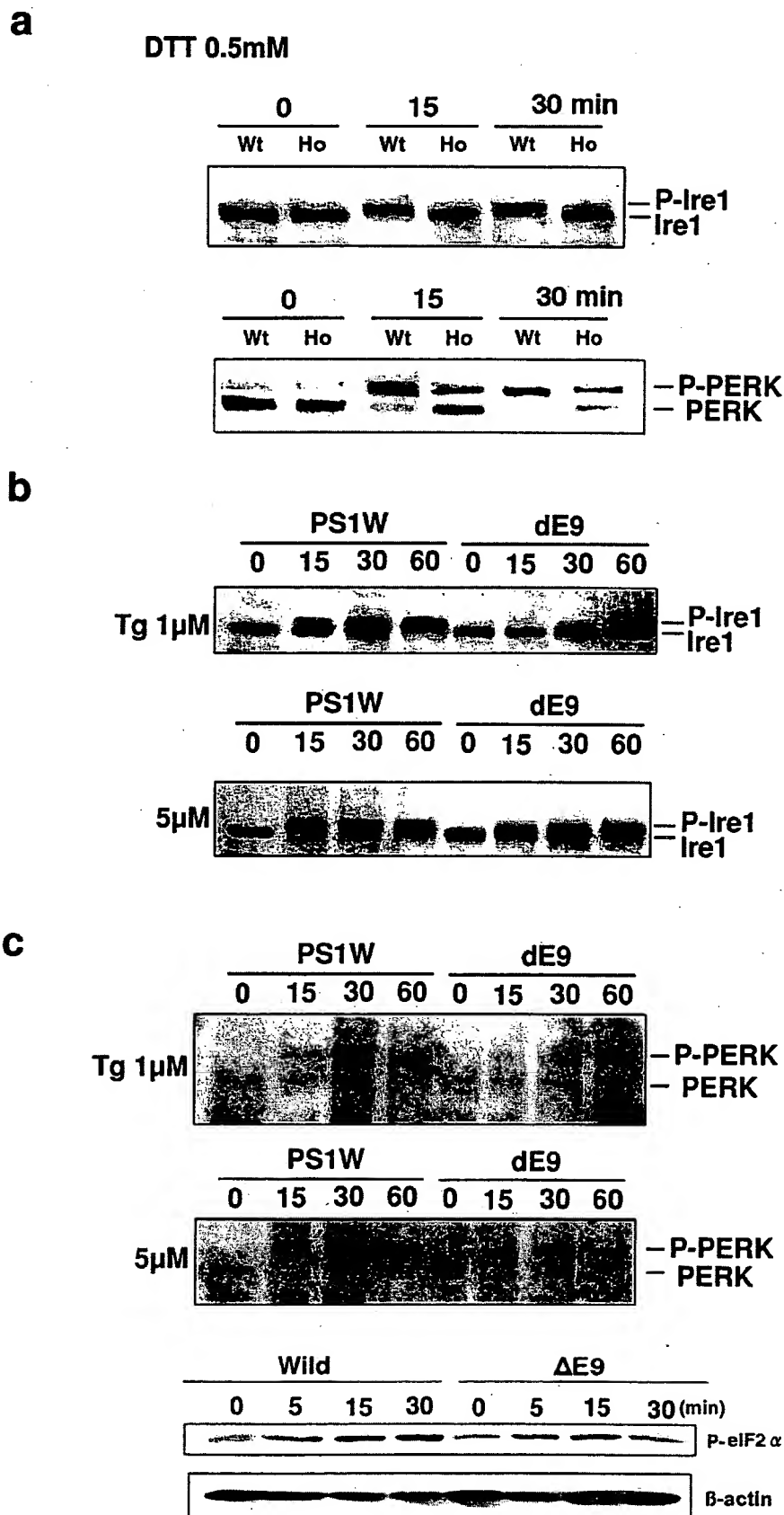
predominantly in the ER, and a small fraction of cells ( $\sim 10\%$ ) showed nuclear staining. Nuclear immunoreactivity of ATF6, which has been demonstrated previously as p50ATF6 fragments (21), increased in wild-type cells from 2 h after the induction of ER stress by treatment with Tm and reached a maximum within 4 h (Fig. 5, *b* and *c*). The changes in ATF6 immunoreactivity were consistent with the results of Western blotting. PS1 mutant knock-in cells showed slight nuclear accumulation of p50ATF6 2 h after induction (Fig. 5, *b* and *c*). After 4 h, it gradually accumulated in the nucleus, and after 8 h, the immunoreactivity was almost equivalent to that in wild-type fibroblasts. Similar findings were obtained in SK-N-SH cells expressing PS1 $\Delta 9$  (Fig. 5c). Thus, mutation in PS1 obviously delayed nuclear accumulation of p50ATF6, which could be ascribed to the delayed processing of p90ATF6 at the ER membrane (see Fig. 4b). In PS1-deficient cells, subcellular localization of ATF6 was not altered compared with that of control cells (Fig. 5c).

**Inhibited Activation of Endogenous ER Stress Transducers by PS1 Mutants**—The above findings demonstrated that PS1 mutants affect the activation of endogenous ATF6 after ER stress. To assess whether functions of the other ER stress transducers, Ire1 $\alpha$  and PERK, are disturbed by PS1 mutants, we examined the activation of these endogenous molecules during ER stress in cells expressing PS1 mutation. Ire1 and PERK activation during ER stress were correlated with autophosphorylation of their cytoplasmic kinase domains. Initially, to examine the effects of PS1 mutants on the activation of Ire1 $\alpha$ , Western blotting was performed using lysates of knock-in fibroblasts stimulated with ER stress inducers. Phosphorylation of Ire1 $\alpha$  retards their mobility on SDS-polyacryl-

amide gels and serves as a convenient marker of their activation status (33). As treatment with Tm inhibits glycosylation of Ire1 $\alpha$ , the retardation of their mobility cannot be detected during ER stress. Therefore, we employed 0.5 mM DTT and 1  $\mu$ M TG as ER stress inducers in this experiment. In wild-type fibroblasts, Ire1 $\alpha$  was completely phosphorylated within 15 min after treatment with DTT (Fig. 6a). In PS1 mutant knock-in cells, almost no phosphorylation of Ire1 $\alpha$  was observed at 15–30 min after treatment. The same findings were observed when cells were treated with 1  $\mu$ M TG (data not shown). Furthermore, the activation of Ire1 $\alpha$  was also inhibited in SK-N-SH cells stably transfected with PS1 mutants when cells were treated with 1  $\mu$ M TG (PS1 $\Delta 9$ , Fig. 6b). These results were consistent with the previous findings of 293T cells transiently co-transfected with Ire1 and PS1 mutants (14), showing that FAD-linked PS1 mutants inhibited autophosphorylation of Ire1 $\alpha$ . The effects of PS1 mutants on inhibited activation of Ire1 $\alpha$  were detected at concentrations from 0.5 to 3  $\mu$ M TG, but no changes were detected at 5  $\mu$ M TG compared with those in cells expressing wild-type PS1 (Fig. 6b). This suggests that higher doses of ER stress inducers could mask the effects of PS1 mutation on the inhibited activation of Ire1, similar to the findings that down-regulation of induction of BiP mRNA was not detected in FAD-linked PS1 mutant-expressing cells at higher doses of ER stress inducers.

Second, we examined the effects of PS1 mutations on activation of PERK. PERK is known as an ER stress signal transducer, which is autophosphorylated and phosphorylates eukaryotic initiation factor-2 $\alpha$  eIF2 $\alpha$  during ER stress (25, 26). PERK was phosphorylated within 15 min after treatment with 0.5 mM DTT in wild-type fibroblasts (Fig. 6a) or 1  $\mu$ M TG (data

**FIG. 6. Inhibited activation of endogenous ER stress transducers.** *a*, fibroblasts from PS1 mutant knock-in mice were treated with 0.5 mM DTT for the indicated times. *Upper panel*, cells were lysed in 1% Triton buffer, and then Western blotting of Ire1 $\alpha$  was carried out. The bands of Ire1 $\alpha$  were shifted to a higher apparent molecular weight after treatment with DTT in wild-type (Wt) fibroblasts. The higher molecular weight bands of Ire1 $\alpha$  were demonstrated to be derived from phosphorylated forms, as described previously (33). *P-Ire1*, phosphorylated-Ire1 $\alpha$ . Phosphorylation of Ire1 $\alpha$  was completely inhibited in homozygous mutant fibroblasts (*Ho*). *Lower panel*, Western blotting of PERK after treatment of fibroblasts with DTT. Phosphorylation of PERK was also inhibited in homozygous mutant fibroblasts. *P-PERK*, phosphorylated-PERK. *b*, SK-N-SH cells stably transfected with each PS1 construct were stimulated with TG (1 and 5  $\mu$ M) for the indicated times, and Western blotting of Ire1 $\alpha$  was performed. When cells were treated with 1  $\mu$ M TG (*upper panel*), the bands of Ire1 $\alpha$  were completely shifted (phosphorylated-Ire1 $\alpha$ ) within 15 min in cells expressing wild-type PS1 (*PS1W*). In contrast, no shift of Ire1 $\alpha$ -immunoreactive bands was seen in  $\Delta$ PS1 cells treated with the same dose of TG. When cells were treated with 5  $\mu$ M TG (*lower panel*), both cells showed that phosphorylation of Ire1 $\alpha$  occurred within 15 min, and there were no differences of the phosphorylation kinetics. *c*, phosphorylation of PERK and eIF2 $\alpha$  in SK-N-SH stable cell lines expressing PS1 constructs. The changes in levels of phosphorylated PERK (*upper and middle panels*) and eIF2 $\alpha$  (*lower panel*) after treatment of cells with 1  $\mu$ M (*upper panel*) and 5  $\mu$ M (*middle*) TG are shown. PS1 mutation inhibited or delayed the phosphorylation of both PERK and eIF2 $\alpha$  after ER stress when cells were treated with 1  $\mu$ M TG treatment, but the differences in phosphorylation kinetics of PERK between wild-type and mutant cells disappeared when cells were treated with 5  $\mu$ M TG.  $\beta$ -Actin was used as an internal control.



not shown). In PS1 mutant knock-in cells, about 50 or 30% of the PERK molecules remained nonphosphorylated at 15 or 30 min, respectively, after ER stress (Fig. 6*a*). In SK-N-SH cells

stably transfected with PS1 mutants ( $\Delta$ PS1), phosphorylation of PERK was severely inhibited within 30 min after treatment with 1  $\mu$ M TG compared with that in cells expressing wild-type

PS1 (Fig. 6c) similar to the findings in PS1 mutation knock-in cells. At 60 min after ER stress, PERK was completely phosphorylated in both wild-type and mutant PS1-expressing cells. These results indicated that activation of PERK was delayed by PS1 mutation at the dose of 1  $\mu$ M TG. When cells were treated with 5  $\mu$ M TG, PERK was completely phosphorylated in these cells within 15 min, indicating that excessive doses of ER stress inducers could mask the effects of PS1 mutation on the delay of activation of PERK.

As described above, the disturbed function of PERK is known to cause the down-regulation of phosphorylation of eIF2 $\alpha$  (25, 26). Therefore, we examined the levels of phosphorylated eIF2 $\alpha$  after ER stress in SK-N-SH cells expressing PS1 mutant. As expected, PS1 mutation inhibited phosphorylation of eIF2 $\alpha$  (Fig. 6c). Thus, activation of PERK and the resultant phosphorylation of eIF2 $\alpha$  were disturbed by expression of a PS1 mutation. Taken together with the results of inhibited activation of Ire1 $\alpha$ , it is possible to conclude that PS1 mutants disturb the signaling pathways from ER stress transducers such as Ire1 $\alpha$ , ATF6, and PERK simultaneously.

#### DISCUSSION

Our recent study showed that a missense mutation in PS1 leads to attenuation of the induction of BiP under ER stress conditions (14). In the present study, to determine whether the function of wild-type PS1 is essential for or is associated with the UPR signaling system, we analyzed the expression of BiP and CHOP, which are known to be induced by ER stress, using PS1-deficient cells. However, we found no attenuation of BiP or CHOP induction in fibroblasts from PS1-deficient mice in contrast to PS1 mutant knock-in cells. Furthermore, the UPR was not down-regulated in cells expressing dominant negative PS1, which was mutated in aspartate at residues 257 or 385. These findings suggest that wild-type PS1 is not associated with UPR signaling. Previously, PS1<sup>-/-</sup> cells were reported to show reduced induction of BiP after ER stress (18). In this paper, it was speculated that the mechanisms of attenuated induction of BiP were due to the disturbance of UPR-dependent proteolytic processing of Ire1 $\alpha$  by a defect in the  $\gamma$ -secretase activity of PS1. We tried to detect the proteolytic processing of Ire1 $\alpha$  and the nuclear accumulation of Ire1 $\alpha$  fragments after ER stress in both normal and PS1-deficient cells. However, we did not observe the cleaved fragments of Ire1 $\alpha$  in both cells. The cause may be attributed to the instability of Ire1 $\alpha$  fragments, i.e. such fragments might be short-lived and therefore difficult to detect. The other possible reason for the nondetection of cleaved fragments of Ire1 $\alpha$  is the differences in experimental conditions, such as methods of cell culture and stimuli by ER stress inducers.

Presenilin proteins seem to be important in the cleavage of APP at the  $\gamma$ -site because inhibition of A $\beta$  production is accompanied by the accumulation of carboxyl-terminal fragments of  $\beta$ -APP in PS1<sup>-/-</sup> cells (11). ATF6 is synthesized as an ER transmembrane protein and is cleaved at or close to the cytosolic face of the membrane. The biochemical characteristics of ATF6 suggest that PS1 may be associated with the cleavage of ATF6 on the ER membrane, similar to the cleavage of APP at the  $\gamma$ -site. However, the conversion of p90ATF6 to p50ATF6 was intact in PS1<sup>-/-</sup> cells, suggesting that PS1 is not associated with the proteolytic process of ATF6, although PS1 has been shown recently to be required for processing of some of the type 1 transmembrane proteins such as APP (11), Notch (34), and Ire1 (18), and that the cleavage is different from the processing of APP at the  $\gamma$ -site. This conclusion was supported by the lack of changes in the processing of ATF6 in cell lines expressing dominant negative PS1 that was mutated in aspartate at residues 257 or 385. In contrast to native PS1, FAD-linked PS1 mutants inhibited the cleavage of p90ATF6. Al-

though the detailed mechanisms are unclear, mutation of PS1 may affect the processing enzymes of ATF6 on the ER membrane. Recently, ATF6 was demonstrated to be processed by Site-1 protease (S1P) and Site-2 protease (S2P), which are processing enzymes known as sterol regulatory element-binding proteins (SREBPs) (35). FAD-linked PS1 mutations have not been reported to inhibit the processing of SREBPs. Therefore, it is inconceivable to consider that FAD-linked PS1 mutants inhibit the activities of S1P and S2P. Ire1 $\alpha$  is known to be sufficient to activate the ATF6 reporter gene, whereas a dominant negative form of Ire1 $\alpha$  blocks ER stress activation (36), suggesting that ATF6 is downstream of Ire1 $\alpha$  in the ER stress signaling pathway. Our study also showed that FAD-linked PS1 mutants inhibited activation of Ire1 $\alpha$ . Taken together, it is likely that disturbances of processing and nuclear transports of ATF6 could be caused by the dysfunction of Ire1 $\alpha$ .

Neither PS1 null nor dominant negative mutants affected the signaling of the UPR. In contrast, FAD-linked PS1 mutants did affect it, suggesting that its abilities could be caused by gaining aberrant function. However, it is unclear whether the effects of mutant PS1 on the UPR could be associated with its  $\gamma$ -secretase activities. To address this issue, a study will need to be made of the ability of PS1 mutants to attenuate the UPR after introducing second mutations into the aspartic acid residues in the catalytic portion of the protein.

The present study has shown that down-regulation of BiP induction by FAD-linked PS1 mutant is due to attenuated signaling of the UPR through decreased levels of phosphorylated Ire1 and inhibition of activation of ATF6 under ER stress conditions. Moreover, PS1 mutants also inhibited the phosphorylation of PERK, which is another ER stress transducer. Therefore, it is possible that mutant PS1 perturbs the functions of each ER stress transducer and inhibits its downstream signal. However, it remains unclear why mutant PS1 inhibits the activation of ER stress transducers. A recent study suggested that activation of the signaling-mediated ER stress transducers could be triggered by dissociation of BiP from stress transducers (33, 36, 37). This dissociation would lead to oligomerization of stress transducers inducing autophosphorylation and the resultant activation of downstream signaling. Previously, we reported that PS1 was associated with Ire1 on the ER membrane (14). If FAD-linked PS1 mutants form malformed structures, BiP may constitutively bind to PS1 molecules to promote its folding. The complex formation of PS1, Ire1 (and/or PERK), and BiP may inhibit the dissociation of BiP from Ire1 (and/or PERK) under ER stress conditions. However, to clarify the detailed mechanisms responsible for perturbation of ER stress signaling by PS1 mutants, further studies focusing on the structures of PS1 molecules bearing missense mutations and the regulation of ER stress sensing are needed.

Sato *et al.* (19) recently reported that FAD-linked PS1 mutations do not have a discernible impact on the ER stress response, a finding that is not consistent with the present study. Their inability to reproduce the previous results, in which we showed that FAD-linked PS1 mutation causes the down-regulation of UPR signaling, is likely to be due to their use of cells (HEK293 and Neuro2a cells) that were, in comparison, not sensitive to ER stress and to their use of time points that were too late. They examined activation of PERK at 5 h after ER stress. As described in our previous study (38) and present studies, FAD-linked PS1 mutants delayed the activation of stress transducers during ER stress, but the effects of PS1 mutations could be masked by treatment with excessive doses of ER stress inducers or stimulation for too long a time. In addition, it is most important to pre-incubate for more than 1 h with fresh medium before treatment with agents to gain

constant data in the ER stress response (as has been described above under "Experimental Procedures"), because the induction levels of BiP mRNA are altered considerably if the changes are not conducted. The decrease of BiP mRNA induction in cells expressing FAD PS1 mutations was ~30 or 50% compared with the controls in the PS1 mutation knock-in fibroblasts or stably transfected SK-N-SH cells, respectively. To detect these subtle defects in the UPR in PS1 mutation-expressing cells, the cells should be handled carefully under the same experimental conditions.

In summary, wild-type PS1 does not play a role in signaling of the UPR, but FAD-linked PS1 mutants do affect it, suggesting that PS1 mutations cause perturbation of the ER stress response through a gain-of-function. The possible mechanism of a perturbed ER stress response could be the inhibition of activation of ER stress transducers such as Ire1 $\alpha$ , ATF6, and PERK. The disturbance of these protective systems to ER stress in PS1 mutation-bearing cells may lead to susceptibility to various cellular stresses.

**Acknowledgments**—We thank Prof. D. Ron (New York University School of Medicine) for antibodies against Ire1 $\alpha$  and PERK and Dr. B. De Strooper (Katholieke Universiteit Leuven and Flanders Institute for Biotechnology) for providing PS1/PS2 double knock-out fibroblasts.

#### REFERENCES

- Selkoe, D. J. (1994) *Annu. Rev. Neurosci.* **17**, 489–517
- Chartier-Harlin, M. C., Crawford, F., Houlden, H., Warren, A., Hughes, D., Fidani, L., Goate, A., Rossor, M., Roques, P., Hardy, J. & Mullan, M. (1991) *Nature* **353**, 844–846
- Goate, A., Chartier-Harlin, M. C., Mullan, M., Brown, J., Crawford, F., Fidani, L., Giuffra, L., Haynes, A., Irving, N., James, L., et al. (1991) *Nature* **349**, 704–706
- Mullan, M., Mullan, M., Crawford, F., Axelman, K., Houlden, H., Lilius, L., Winblad, B. & Lannfelt, L. (1992) *Nat. Genet.* **1**, 345–347
- Sherrington, R., Rogaev, E. I., Liang, Y., Rogaeva, E. A., Levesque, G., Ikeda, M., Chi, H., Lin, C., Li, G., Holman, K., Tsuda, T., Mar, L., Foncin, J.-F., Bruni, A. C., Montesi, M. P., et al. (1995) *Nature* **375**, 754–760
- Levy-Lahad, E., Wijsman, E. M., Nemens, E., Anderson, L., Goddard, K. A., Weber, J. L., Bird, T. D. & Schellenberg, G. D. (1995) *Science* **269**, 970–973
- Levy-Lahad, E., Wasco, W., Poorkaj, P., Romano, D. M., Oshima, J., Pettingell, W. H., Yu, C. E., Jondro, P. D., Schmidt, S. D., Wang, K., Crowley, A. C., Fu, Y.-H., Guenette, S. Y., Galas, D., Nemens, E., et al. (1995) *Science* **269**, 973–977
- Rogaev, E. I., Sherrington, R., Rogaeva, E. A., Levesque, G., Ikeda, M., Liang, Y., Chi, H., Lin, C., Holman, K., Tsuda, T., Mar, L., Sorbi, S., Nacmias, B., Piacentini, S., Amaducci, L., et al. (1995) *Nature* **376**, 775–778
- Borchelt, D. R., Thinakaran, G., Eckman, C. B., Lee, M. K., Davenport, F., Ratovitsky, T., Prada, C. M., Kim, G., Seekins, S., Yager, D., Slunt, H. H., Wang, R., Seeger, M., Levey, A. I., Gandy, S. E., Copeland, N. G., Jenkins, N. A., Price, D. L., Younkin, S. G. & Sisodia, S. S. (1996) *Neuron* **17**, 1005–1013
- Duff, K., Eckman, C., Zehr, C., Yu, X., Prada, C. M., Perez-tur, J., Hutton, M., Buee, L., Harigaya, Y., Yager, D., Morgan, D., Gordon, M. N., Holcomb, L., Refolo, L., Zenk, B., Hardy, J. & Younkin, S. (1996) *Nature* **383**, 710–713
- De Strooper, B., Saftig, P., Craessaerts, K., Vanderstichele, H., Guhde, G., Annaert, W., Figura, K. V. & Leuven, F. V. (1998) *Nature* **391**, 387–390
- Guo, Q., Sopher, B. L., Furukawa, K., Pham, D. G., Robinson, N., Martin, G. M. & Mattson, M. P. (1997) *J. Neurosci.* **17**, 4212–4222
- Guo, Q., Fu, W., Sopher, B. L., Miller, M. W., Ware, C. B., Martin, G. M. & Mattson, M. P. (1999) *Nat. Med.* **5**, 101–106
- Katayama, T., Imaizumi, K., Sato, N., Miyoshi, K., Kudo, T., Hitomi, J., Morihara, T., Yoneda, T., Gomi, F., Mori, Y., Nakano, Y., Takeda, J., Tsuda, T., Itoyama, Y., Murayama, O., Takashima, A., St. George-Hyslop, P., Takeda, M. & Tohyama, M. (1999) *Nat. Cell Biol.* **1**, 479–485
- Sidrauskis, C., Chapman, R. & Walter, P. (1998) *Trends Cell Biol.* **8**, 245–249
- Tirasophon, W., Welihinda, A. A. & Kaufman, R. J. (1998) *Genes Dev.* **12**, 1812–1824
- Wang, X.-Z., Harding, H. P., Zhang, Y., Jolicoeur, E. M., Kuroda, M. & Ron, D. (1998) *EMBO J.* **17**, 5708–5717
- Niwa, M., Sidrauskis, C., Kaufman, R. J. & Walter, P. (1999) *Cell* **99**, 691–702
- Sato, N., Urano, F., Yoon, Leem, Y. J., Kim, S. H., Li, M., Donoviel, D., Bernstein, A., Lee, A. S., Ron, D., Veselits, M. L., Sisodia, S. S. & Thinakaran, G. (2000) *Nat. Cell Biol.* **2**, 863–870
- Yoshida, H., Haze, K., Yanagi, H., Yura, T. & Mori, K. (1998) *J. Biol. Chem.* **273**, 33741–33749
- Haze, K., Yoshida, H., Yanagi, H., Yura, T. & Mori, K. (1999) *Mol. Biol. Cell* **10**, 3787–3799
- Yoshida, H., Okada, T., Haze, K., Yanagi, H., Yura, T., Negishi, M. & Mori, K. (2000) *Mol. Cell Biol.* **20**, 6755–6767
- Roy, B. & Lee, A. S. (1999) *Nucleic Acids Res.* **27**, 1437–1443
- Wolfe, M. S., Xia, W., Ostaszewski, B. L., Diehl, T. S., Kimberly, W. T. & Selkoe, D. J. (1999) *Nature* **398**, 513–517
- Harding, H. P., Zhang, Y. & Ron, D. (1999) *Nature* **397**, 271–274
- Harding, H. P., Zhang, Y., Bertolotti, A., Zeng, H. & Ron, D. (2000) *Mol. Cell* **5**, 897–904
- Shen, J., Bronson, R. T., Chen, D. F., Xia, W., Selkoe, D. J. & Toneyawa, S. (1997) *Cell* **89**, 629–639
- Wong, P. C., Zheng, H., Chen, H., Becher, M. W., Sirinathsinghji, D. J., Trumbauer, M. E., Chen, H. Y., Price, D. L., Van der Ploeg, L. H. & Sisodia, S. S. (1997) *Nature* **387**, 288–292
- Herreman, A., Hartmann, D., Annaert, W., Saftig, P., Craessaerts, K., Serneels, L., Umans, L., Schrijvers, V., Checler, F., Vanderstichele, H., Baekelandt, V., Dressel, R., Cupers, P., Huylebroeck, D., Zwijsen, A., Van Leuven, F. & De Strooper, B. (1999) *Proc. Natl. Acad. Sci. U. S. A.* **96**, 11872–11877
- Nakano, Y., Kondoh, G., Kudo, T., Imaizumi, K., Kato, M., Miyazaki, J. I., Tohyama, M., Takeda, J. & Takeda, M. (1999) *Eur. J. Neurosci.* **11**, 2577–2581
- Wang, X. Z., Lawson, B., Brewer, J. W., Zinszner, H., Sanjay, A., Mi, L. J., Boorstein, R., Kreibich, G., Hendershot, L. M. & Ron, D. (1996) *Mol. Cell Biol.* **16**, 4273–4280
- Kaufman, R. J. (1999) *Genes Dev.* **13**, 1211–1233
- Bertolotti, A., Zhang, Y., Hendershot, L. M., Harding, H. P. & Ron, D. (2000) *Nat. Cell Biol.* **2**, 326–332
- De Strooper, B., Annaert, W., Cupers, P., Saftig, P., Craessaerts, K., Mumm, J. S., Schroeter, E. H., Schrijvers, V., Wolfe, M. S., Ray, W. J., Goate, A. & Kopan, R. (1999) *Nature* **398**, 518–522
- Ye, J., Rawson, R. B., Komuro, R., Chen, X., Dave, U. P., Prywes, R., Brown, M. S. & Goldstein, J. L. (2000) *Mol. Cell* **6**, 1355–1364
- Wang, Y., Shen, J., Arenzana, N., Tirasophon, W., Kaufman, R. J. & Prywes, R. (2000) *J. Biol. Chem.* **275**, 27013–27020
- Liu, C. Y., Schroder, M. & Kaufman, R. J. (2000) *J. Biol. Chem.* **275**, 24881–24885
- Imaizumi, K., Katayama, T. & Tohyama, M. (2001) *Nat. Cell Biol.* **3**, E104



**This Page is Inserted by IFW Indexing and Scanning  
Operations and is not part of the Official Record**

**BEST AVAILABLE IMAGES**

Defective images within this document are accurate representations of the original documents submitted by the applicant.

Defects in the images include but are not limited to the items checked:

- ☒ **BLACK BORDERS**
- ☐ **IMAGE CUT OFF AT TOP, BOTTOM OR SIDES**
- ☐ **FADED TEXT OR DRAWING**
- ☐ **BLURRED OR ILLEGIBLE TEXT OR DRAWING**
- ☐ **SKEWED/SLANTED IMAGES**
- ☐ **COLOR OR BLACK AND WHITE PHOTOGRAPHS**
- ☐ **GRAY SCALE DOCUMENTS**
- ☒ **LINES OR MARKS ON ORIGINAL DOCUMENT**
- ☐ **REFERENCE(S) OR EXHIBIT(S) SUBMITTED ARE POOR QUALITY**
- ☐ **OTHER: \_\_\_\_\_**

**IMAGES ARE BEST AVAILABLE COPY.**

**As rescanning these documents will not correct the image problems checked, please do not report these problems to the IFW Image Problem Mailbox.**